*energies*

MDPI

*Article*

# Enlightening Load Modeling by Means of Power Factor Decompositions

**Helmo K. Morales Paredes [1,*], Matheus Branco Arcadepani [1], Alexandre Candido Moreira [2], Flávio A. Serrão Gonçalves [1] and Fernando Pinhabel Marafão [1]**

[1] Institute of Science and Technology of Sorocaba, São Paulo State University (UNESP), Av. Três de Março 511, Sorocaba 18087-180, SP, Brazil
[2] Centre of Innovation, Research and Teaching in Mechatronics, Federal University of Sao Joao del-Rei (UFSJ), Rod.: MG 443, KM 7, Ouro Branco 36494-899, MG, Brazil
* Correspondence: helmo.paredes@unesp.br; Tel.: +55-153-238-3478

**Abstract:** Considering the proliferation of power electronics applications and distributed energy resources, modern power grids are facing a significant increase in harmonic currents circulation and supply voltage deterioration, occasionally associated with small frequency variations. In such a context, the understanding of power phenomena in circuits with linear and non-linear loads under non-sinusoidal voltage conditions is nontrivial and still does not allow for an easy interpretation of harmonic sources, harmonic power flow or the identification of the parameters of a proper equivalent circuit. The main challenge is to develop modern theoretical approaches for load characterization, modeling, and parameter estimation so that new techniques can be formulated to provide adequate guiding for the analysis, compensation, revenue metering, accountability and other applications of power systems. Thus, based on the Conservative Power Theory (CPT) and further decomposition of its apparent power and power factor definitions, this paper proposes a novel methodology for estimating equivalent parameters and for proposing proper equivalent circuits capable of representing/modeling the main characteristics of single-phase generic loads (black boxes) and the related power phenomena in terms of passive dipoles (linear loads) or of harmonic voltage/current sources and their intrinsic transimpedances/transadmittances (non-linear loads). Simulation and experimental results were depicted to support and validate the proposed approach, showing that it might be a powerful modeling technique to represent generic loads in a modern power grid scenario, while being used for complex applications such as reactive power compensation or accountability in circuits with nonlinear loads and distorted voltages.

**Keywords:** equivalent circuits; harmonic distortion; load modeling; non-linear loads; power factor; revenue metering



**Citation:** Paredes, H.K.M.; Arcadepani, M.B.; Moreira, A.C.; Gonçalves, F.A.S.; Pinhabel Marafão, F. Enlightening Load Modeling by Means of Power Factor Decompositions. *Energies* **2023**, *16*, 4089. https://doi.org/10.3390/en16104089

Academic Editors: Ioana-Gabriela Sirbu and Lucian Mandache

Received: 9 February 2023
Revised: 22 March 2023
Accepted: 3 April 2023
Published: 15 May 2023



## 1. Introduction

Due to the proliferation of electronic power converters widely applied in industrial, commercial, and residential installations, modern power grids are facing a significant increase in the circulation of harmonic currents. Consequently, supply voltage deterioration causes different problems for utilities and operation by end-users [1–6]. Such a scenario could be even more complex in power grids with distributed energy resources [7–9] on which the grid frequency can slightly vary, and the voltage distortions cannot always be neglected [1,2] for the bidirectional power flow [9]. In this context, beyond adopting more stringent standards, the main challenge is to develop advanced techniques for load characterization, modeling, and parameter estimation so that novel approaches can be formulated to provide adequate guidance for power system design, compensation, revenue metering, accountability and other electrical engineering processes. For this reason, adapting or enhancing the concepts of modern power theories [10–13] to this new environment is mandatory.

For more than a century, AC circuit analysis has been based on complex algebra, such as that proposed by Steinmetz [14], but the broader validity of these concepts have been challenged ever since [10,11,15]. In this sense, various methods have been developed to generalize classic active/reactive/apparent power concepts. Time-domain methods [11,12,16,17], frequency-domain methods [13,18,19] and other proposals were formulated [10,20–23] and some exciting comparative studies can be found in [24–29].

All these proposals have contributed greatly to our understanding of the modeling and analysis of linear and non-linear circuits. However, the investigation of power phenomena under non-sinusoidal voltage conditions is nontrivial, and it still does not allow for easy interpretation of harmonic sources, harmonic power flow, or the identification of real load parameters.

In this context, an important matter is verifying the behavior of non-linear loads and determining whether they should be represented as "harmonic voltage sources" or "harmonic current sources" [30,31], making possible their modeling and analysis for feature extraction, the mitigation of power quality (PQ) problems [3,6,32–34] and the assignment of responsibilities between utilities and end-users on the generation of disturbances and energy flow [35–39]. As discussed in [6], household appliances containing motors and transformers, such as refrigerators, freezers, washing machines, and air conditioning devices may be characterized as harmonic current source (HCS) loads. These loads are characterized by a high reactive power demand and a current waveform distortion, which causes the phase shift between the voltage and current and harmonics production. In contrast, electronic devices containing a rectifier stage with capacitive output (DC) filter, which leads to distorting the current and low power factor, may be characterized as harmonic voltage source (HVS) loads. Some examples are battery chargers, TV sets, electronic ballasts, microwaves, etc. These HCS and HVS loads can cause voltage distortion, which can lead to reduced power quality, increased power demand, a lower power factor, and higher energy bills, and can also cause voltage spikes, surges or notches due to their switching behavior. Such voltage deterioration can damage sensitive equipment and cause equipment malfunction [4,5,13,32].

To characterize different aspects of the load operation, the authors in [40] defined a set of load performance indexes based on the Conservative Power Theory (CPT). These indexes were based on CPT power decomposition and have a direct relation to the power factor definition. Later, in [35], the authors proposed a load characterization and revenue-metering approach using CPT decompositions and symmetrical components, focusing on estimating the power accountable to the load, apart from the effects of line impedances and the deterioration of the source voltage on the point of common coupling (PCC). However, although the concept of power factor decomposition has been indirectly addressed in [40], neither their physical representations from the load point of view nor the estimation of the load parameters were presented, and no experimental verification was presented either.

With all this in mind and expanding the approaches presented in [35,40], this paper aims at discussing the decomposition and physical meaning of the load power factor, which allows not only for obtaining the load behavior but also the complete characterization of the loads, with the estimation of their parameter as a function of the fundamental voltage and/or current components. Hence, the proposed approach drives load modeling from its general context, where the loads are considered as "black boxes," and also enables the analysis of harmonic power flow.

Moreover, while in [35,40] the revenue-metering problem was discussed by comparing the actual load operation with a very basic load modeling approach to infer the power terms accountable to the load, now the approach has been completely revised, extended and enlightened. The power factor decomposition into load conformity factors not only allows for a full understanding of the process of current distortion and reactive power generation, but also provides a powerful tool for estimating the load parameters, i.e., an Equivalent Circuit (EC) that reproduces, with maximum effectiveness, the operation of actual load. This is the main requirement for an approach with proper accountability,

splitting the power accountable to the load from the terms that should be ascribed to supply non-idealities.

Thus, Section 2 presents the original CPT-based circuits for the discussion of load characterization, as well as the development of new general equivalent circuits derived from power factor decomposition, while the relationship among the power factor components and the proposed methodology for estimating the load parameters is discussed in Section 3. Then, based on simulation and laboratory tests obtained from several studies, the harmonic power flow, load characterization and load parameter estimations are analyzed and discussed in Section 4. Conclusions are presented in Section 5.

## 2. Load Modeling and Characterization under Generic Supply Conditions

### *2.1. Fundamental Definitions and CPT-Based Equivalent Circuits*

The modeling of a generic load involves analyzing its behavior under generic voltage waveforms and the CPT, presented in [12,35], which provides a particularly good approach. Thus, the basic CPT definitions are subsequently recalled and considered as references for reactive energy and orthogonal current decompositions in single-phase circuits.

The reactive energy $W_r$ at a given port was defined as:

$$W_r = \frac{1}{T}\int_0^T \hat{v}.idt, \tag{1}$$

Here $i$ is the current and $\hat{v}$ is the unbiased voltage integral (see Appendix A).

Hence, based on the reactive energy definition, a generic (linear/non-linear) load can be modeled by the equivalent circuits of Figure 1 [35], according to one of the following possibilities:

- If $W_r$ is positive (+), the load can be modeled by a parallel arrangement of an equivalent conductance ($G_e$), an equivalent inductor ($L_e$) and a harmonic current source ($j_e$) representing the harmonics produced by the energy conversion in the load side (Figure 1a).
- If $W_r$ is negative (−), the load can be modeled by a series arrangement of an equivalent resistance ($R_e$), an equivalent capacitor ($C_e$), and a harmonic voltage source ($u_e$) representing the harmonics produced by the energy conversion in the load side (Figure 1b).

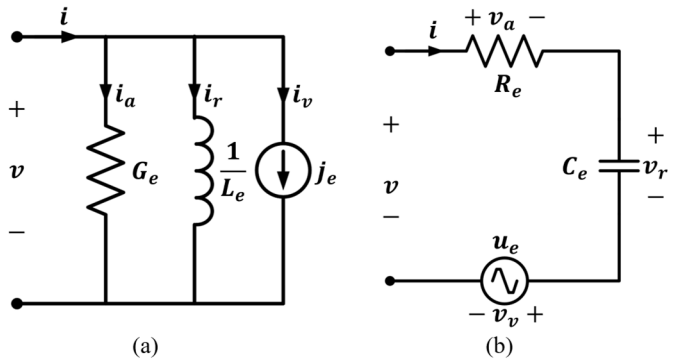


**Figure 1.** CPT load modeling under non-sinusoidal conditions. (**a**) $W_r > 0$; (**b**) $W_r < 0$.

Thus, for a generic load modeled by the equivalent circuit shown in Figure 1a, the current is given by:

$$i = G_e v + \frac{1}{L_e}\hat{v} + j_e \equiv i_a + i_r + i_v, \tag{2}$$

where:

- $i_a = G_e v = \frac{P}{V^2} v$ is the active current, such that $P$ is the active power, $V$ is the voltage RMS value and $G_e$ is the equivalent conductance [$\Omega^{-1}$]. Therefore, $G_e$ is the inverse of equivalent resistance $R_e$ [$\Omega$].

- $i_r = \frac{1}{L_e}\hat{v} = \frac{W_r}{\hat{V}^2}\hat{v}$ is the reactive current, $\hat{V}$ is the RMS value of $\hat{v}$ and $L_e$ is the equivalent inductance [H].
- $i_v = j_e = i - i_a - i_r$ is the void current and represents the remaining current that does not transfer active power nor reactive energy.

On the other hand, for a load modeled by the equivalent circuit shown in Figure 1b, the voltage is given by:

$$v = R_e i + \frac{1}{C_e}\hat{i} + u_e \equiv v_a + v_r + v_v, \tag{3}$$

where $v_a = R_e i$ is active voltage, $v_r = \frac{1}{C_e}\hat{i} = \frac{V^2}{|-Wr|}\hat{i}$ is reactive voltage, $C_e$ is the equivalent capacitance [F], $v_v = u_e = v - v_a - v_r$ is the void voltage and $\hat{i}$ is the unbiased current integral (see Appendix A). Notice that the circuits in Figure 1 are more general than those proposed in [30,31], where the concepts of load voltage source type and current source type have been introduced for non-linear loads.

Considering that decomposition in (2) and (3) is orthogonal, the RMS values of voltage and current terms can be associated as:

$$I = \sqrt{I_a^2 + I_r^2 + I_v^2}, \tag{4a}$$

$$V = \sqrt{V_a^2 + V_r^2 + V_v^2}, \tag{4b}$$

Other relevant information to characterize load operating conditions at a given port are the apparent power and power factor:

$$A = V\sqrt{I_a^2 + I_r^2 + I_v^2} \equiv \sqrt{P^2 + Q^2 + D^2}, \tag{5}$$

$$\lambda = \frac{P}{A} = \frac{P}{\sqrt{P^2 + Q^2 + D^2}}, \tag{6}$$

where the power terms can be defined as:

$$P = VI_a \equiv G_e V^2 \text{ activepower} \tag{7a}$$

$$Q = VI_r \equiv W_r \xrightarrow[\hat{V}]{V} \text{ reactivepower} \tag{7b}$$

$$D = VI_v \text{ void (distortion) power} \tag{7c}$$

Moreover, owing to the reactive energy nature (inductive or capacitive) and the voltage distortion, the reactive power $Q$ can be expressed as:

$$Q = VI_r \text{sign}(W_r) \equiv \omega(1 + \sigma_v)W_r, \tag{8}$$

where $\omega$ is the angular line frequency and $\sigma_v$ is the voltage distortion factor (Appendix A). Notice that the reactive power is proportional to reactive energy, but it also depends on line frequency and voltage distortion.

Moreover, such power and power factor definitions provide a good understanding of relevant physical phenomena, such as power consumption, energy storage and harmonic power flow. For this reason, additional power factor decomposition is applied in the following sections with the purpose of collecting meaningful information for load modeling through equivalent dipoles.

### *2.2. Enhancements of Equivalent Circuits for Load Modeling*

Although the parameter estimation and equivalent circuits from the last section represent a solid approach for several applications [3,12,32–35,40], the authors were seeking for an alternative way of demonstrating the effects of voltage distortions and load nonlinearities on the equivalent circuit parameters. Thus, making use of the equivalent inductance, $L_e$, it is possible to show that reactive power can be expressed by:

$$Q = \omega(1 + \sigma_v)W_r \equiv \frac{1}{\omega L_e(1 + \sigma_v)}V^2 = \frac{B_{eL}}{1 + \sigma_v}V^2, \tag{9}$$

such that $B_{eL} = \frac{1}{\omega L_e}$ is the generalized inductive equivalent susceptance [S].

The void (distortion) power can also be expressed by:

$$D = VI_v \equiv Y_{ei}V^2, \tag{10}$$

such that $Y_{ei} = \frac{I_v}{V}$ is the equivalent transadmittance measured in [S], which represents the scattering harmonic current stemming from the interaction of the supplying voltage harmonics with the load transadmittance (i.e., currents accounted due to the different values of equivalent admittance at different harmonics) and generated harmonics (i.e., current harmonics that do not exist in the voltage spectrum).

From (6), (7), (9) and (10), we can therefore express the power factor as:

$$\lambda = \frac{I_a}{\sqrt{I_a^2 + I_r^2 + I_v^2}} \equiv \frac{G_e}{\sqrt{G_e^2 + \left(\frac{B_{eL}}{1+\sigma_v}\right)^2 + Y_{ei}^2}}, \tag{11}$$

which can be calculated for any circuit independently of waveform distortion and is affected not only by energy storage or non-linear dipoles, but also by voltage distortions. Thus, the previous definitions establish a consistent basis for analyzing and interpreting the power phenomena with linear and non-linear loads under generic supply conditions.

Therefore, (11) shows that the load model presented in Figure 1 can be reconsidered using the generic equivalent dipoles of Figure 2, where a generic load can be modeled by a *current components-based circuit* (Figure 2a), in case of inductive behavior; or by a *voltage components-based circuit* (Figure 2b), in case of capacitive behavior. The series connection of Figure 2b (dual to the parallel circuit shown in Figure 2a) can be achieved by using (4b), the active power $P$, reactive power $Q$ and void (distortion) power $D$:

$$P = IV_a \equiv R_e I^2, \tag{12a}$$

$$Q = IV_r \equiv \frac{1}{B_{eC}(1+\sigma_i)} I^2, \tag{12b}$$

$$D = IV_v \equiv Z_{ev} I^2, \tag{12c}$$

where $B_{eC} = \omega C_e$ is the generalized capacitive equivalent susceptance [S], $\sigma_i$ is the current distortion factor (Appendix A) and $Z_{ev} = \frac{V_v}{I}$ is the equivalent transimpedance measured in [Ω], which represents the energy conversion from supplying voltage harmonics to other uncommon voltage harmonics.

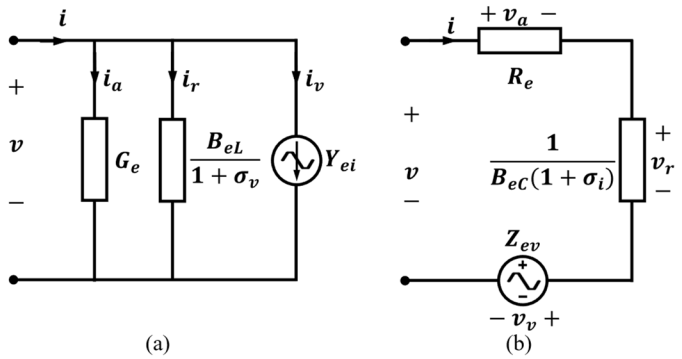


**Figure 2.** General load modeling based on power factor decomposition: (**a**) current components-based circuit; (**b**) voltage components-based circuit.

Notice that the improved equivalent circuits of Figure 2 make it possible to understand and evaluate the impact of supplying voltage distortions on the equivalent circuit parameters. Moreover, load nonlinearities are modeled as current/voltage source linked to the voltage supply with a magnitude depending on a proper transadmittance ($Y_{ei}$) or transimpedance ($Z_{ev}$) parameter.

*2.3. Power Factor Decomposition in Terms of Equivalent Circuit Parameters*

To characterize the different aspects of a generic load operation on the power factor, novel performance indexes were proposed in [40]. However, they were not investigated in detail after being proposed. Consequently, based on the above definitions, these conformity (performance) indexes are reformulated herein by using the proposed equivalent parameters (dipoles) and well-known PQ indices such as $THD_I = \sum_{h=2}^{\infty} I_h / I_1$ (subscripts "h" and "1" indicate harmonic order and the fundamental component) and the displacement factor ($\cos\phi$). As a result, the conformity factors can be calculated regardless of the current and voltage waveforms.

- Reactivity factor ($\lambda_Q$): knowing that the reactive current is related to the phase displacement between voltage and current in the various frequencies, similarly to the traditional $\cos\phi$ applied to sinusoidal signals (voltage and current). This conformity factor can be used to generalize the displacement effect for non-sinusoidal voltage and current conditions:

$$\lambda_Q = \frac{I_r}{\sqrt{I_a^2 + I_r^2}} \equiv \frac{\frac{B_{eL}}{1+\sigma_v}}{\sqrt{{G_e}^2 + \left(\frac{B_{eL}}{1+\sigma_v}\right)^2}}, \tag{13}$$

It should be noted that, irrespective of the frequency variation and voltage distortion, $\lambda_Q$ indicates the phase displacement between voltages and currents caused by energy storage elements (inductors and capacitors) or by non-linear dipoles. Notice that $\lambda_Q$ vanishes only if the reactive current is reduced to zero ($i_r = 0$).

In case of inductive loads, the capacitance required for total compensation, results in:

$$C_e = \frac{W_r}{V^2} = -\frac{1}{L_e}\frac{\hat{V}^2}{V^2} = \frac{-B_{eL}}{\omega(1+\sigma_v)^2} \Rightarrow B_{eC} = \frac{-B_{eL}}{(1+\sigma_v)^2}, \tag{14}$$

- Non-linearity (distortion) factor ($\lambda_D$): as the void current contains all the harmonic components that do not generate active or reactive energy, this factor can be used to calculate the distortion index, as follows:

$$\lambda_D = \frac{I_v}{\sqrt{I_a^2 + I_r^2 + I_v^2}} \equiv \frac{Y_{ei}}{\sqrt{G_e^2 + \left(\frac{B_{eL}}{1+\sigma_v}\right)^2 + Y_{ei}^2}}, \tag{15}$$

Again, $\lambda_D$ vanishes only if the void current is reduced to zero ($i_v = 0$).

- Lastly, from (11), (13) and (15), it can be demonstrated that the load power factor ($\lambda$) can be expressed as:

$$\lambda = \frac{G_e}{\sqrt{G_e^2 + \left(\frac{B_{eL}}{1+\sigma_v}\right)^2 + Y_{ei}^2}} \equiv \sqrt{\left(1-\lambda_Q^2\right)\left(1-\lambda_D^2\right)} \tag{16}$$

From (16) it is possible to correlate and quantitatively evaluate the effect of each dipole from the load equivalent circuit to the power factor. Furthermore, (16) also shows that the power factor is unitary only if the load is purely resistive, regardless of the input voltage.

Thus, the previous definitions give a physical sense to the power factor and each conformity factor, current and power terms, providing a simple technique to describe a generic load (black box) by estimating the equivalent parameters as in Figure 2, which might be influenced by voltage distortions in weak grids or microgrids. Indeed, these systems may experience an increased voltage harmonic content [1–3]. Therefore, the PCC voltages cannot give enough information to identify the real parameters estimation of the "black box" (generic load) under distortion voltage conditions. A proper metering approach should be capable of depurating the effects of supply nonideality, ensuring that the loads are modeled only by their own parameters. Thus, the goal of the following load characterization approach is to identify the real load parameters.

## 3. Proposed Approach for Estimation of Load Parameters

The central idea of this novel approach is to extract an equivalent load model from the load conformity factors defined in the previous section, which represents a "black box" (generic) load. Thus, it is necessary to discriminate the influence of source and load effects on the generation of the unwanted terms of the current/power. In fact, voltage harmonics can be generated by either non-linear loads or distorted supply voltages. Therefore, assuming that the supply voltage should be sinusoidal, the conformity factors defined in (13), (15) and (16) result in (17), (19) and (20).

$$\lambda_Q = \frac{\frac{1}{\omega L_1}}{\sqrt{G_1^2 + \left[\frac{1}{\omega L_1}\right]^2}} = \frac{B_{L1}}{\sqrt{G_1^2 + B_{L1}^2}} \cong \sin\phi \tag{17}$$

In addition, the capacitor (at fundamental frequency) needed for a total reactive compensation result:

$$\omega C_1 = -\frac{1}{\omega L_1} \Rightarrow \omega C_1 = B_{C1} = -B_{L1} \tag{18}$$

In the case of $\lambda_D$, it may still be associated with the traditional current $THD$, by:

$$\lambda_D = \frac{Y_{\ell i}}{\sqrt{G_1^2 + {B_1}^2 + Y_{\ell i}^2}} \equiv \frac{THD_I}{\sqrt{1 + THD_I^2}} \tag{19}$$

where, $Y_{\ell i} = \frac{I_{h\ell}}{V_1}$ is the load transadmittance [S], which represents the harmonic currents, generated by non-linear loads and $I_{h\ell}$ is the rms value of the harmonic current generated by the load.

Finally, the power factor results:

$$\lambda = \frac{G_1}{\sqrt{G_1^2 + {B_1}^2 + Y_{\ell i}^2}} \equiv \cos\phi \sqrt{\left(\frac{1}{1 + THD_I^2}\right)} \tag{20}$$

Therefore, from (20), the parameters of the black box (generic load) can be characterized by a parallel arrangement of dipoles as shown in Figure 3a, which represents an inductive behavior with positive reactive energy ($W_{r1} > 0$). If the generic load feature presents capacitive behavior, reactive energy becomes negative ($W_{r1} < 0$) and the parallel connection can be replaced by the series connection of Figure 3b.

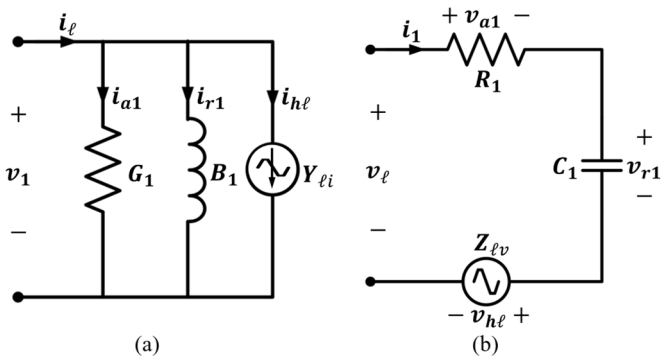


**Figure 3.** Equivalent circuit after load parameter estimation: (**a**) harmonic current source; (**b**) harmonic voltage source.

Observe that, unlike the equivalent circuits shown in Figures 1 and 2, Figure 3 represents the real parameter of the load, so that approach provides a more suitable characterization for the generic load, where the parallel circuit is composed of a fundamental equivalent conductance ($G_1$), a fundamental equivalent susceptance ($B_1$), and a harmonic current source ($i_{h\ell}$). In contrast, the series circuit is composed of a fundamental equivalent resistance ($R_1$), a fundamental equivalent capacitor ($C_1$), and a harmonic voltage source

($v_{h\ell}$). In this case, voltage and current source ($v_{h\ell}$ and $i_{h\ell}$) indicate the harmonics coming from load energy conversion (harmonics generated by the load).

Considering the equivalent circuits of Figure 3 and assuming that the measuring equipment (i.e., PQ monitor, electronic meter, smart inverter, etc.) at the load terminals is capable of decomposing the fundamental ($v_1$, $i_1$) and harmonic ($v_h$, $i_h$) components of the voltages and currents, the parameters of the equivalent circuit for the characterization of a generic load are calculated to suit the circuit performance at the fundamental frequency, thus:

- Fundamental conductance [S]:

$$G_1 = \frac{P_1}{V_1^2} = \frac{1}{R_1} \tag{21}$$

- Fundamental inductive susceptance [S]:

$$\frac{1}{L_1} = \frac{W_{r1}}{\hat{V}_1^2} = \frac{\omega^2 Q_1}{\omega V_1^2} \Rightarrow \frac{1}{\omega L_1} = B_{L1} = \frac{Q_1}{V_1^2} \tag{22}$$

Since $G_1$ and $L_1$ are supplied by a fundamental voltage ($v_1$), they must absorb exactly the fundamental load current ($i_1$). Thus:

$$i_1 = G_1 v_1 + \frac{1}{L_1}\hat{v}_1 \tag{23}$$

- Harmonic current source [A]:

$$i_{h\ell} = i_\ell - G_1(v_1 + v_h) - \frac{1}{L_1}(\hat{v}_1 + \hat{v}_h) \tag{24a}$$

$$i_{h\ell} = i_\ell - i_1 - G_1 v_h - \frac{1}{L_1}\hat{v}_h = i_h - G_1 v_h - \frac{1}{L_1}\hat{v}_h \tag{24b}$$

where, $i_\ell$ is the current accountable to the load.

The same idea can be applied to the series circuit.

- Fundamental resistance [Ω]:

$$R_1 = \frac{P_1}{I_1^2} = \frac{1}{G_1} \tag{25}$$

- Fundamental capacitive susceptance [F]:

$$C_1 = -\frac{\hat{I}_1^2}{W_{r1}} = -\frac{\omega I_1^2}{\omega^2 Q_1} \Rightarrow \omega C_1 = \frac{I_1^2}{Q_1} = B_{C1} \tag{26}$$

- Harmonic voltage source [V]:

$$v_{h\ell} = v_1 - R_1 i_\ell - \frac{\hat{i}_\ell}{C_1} = v_h - R_1 i_h - \frac{\hat{i}_h}{C_1} \tag{27}$$

Clearly, one can see that both current and voltage sources are due to the harmonic components in the current and voltage waveforms, as well as their harmonic portions of unbiased integrals. Thus, with the identified parameters, it is possible to describe the equivalent circuit that characterizes a generic load. Moreover, the equivalent circuits (Figure 3) could be especially useful or necessary to different applications, such as PQ assessment and mitigation, disturbing load identification, harmonic propagation studies, revenue metering and accountability. Moreover, these quantities can be evaluated directly in the time domain and can be measured by simple instrumentation.

## 4. Simulation and Experimental Validation

The main intention in choosing the study cases was to demonstrate how the proposed modeling approach can estimate equivalent circuit parameters, capable of representing/modeling linear and/or non-linear loads, by means of passive dipoles or voltage/current harmonic sources (active dipoles). Thus, very simple circuits (practical or not) were selected for the computer simulations, which are powerful enough in terms of power phenomena interpretation and estimation of the equivalent circuit. For the experimental

validation, two simple, practical loads were chosen, for which the operating conditions were sufficient for validating the modeling approach in terms of the CPT power-based equivalent parameters and their direct association and interpretation in terms of the power factor decomposition.

Therefore, considering a set of generic linear and non-linear loads under sinusoidal and non-sinusoidal voltage conditions, several studies were carried out to illustrate the proposed power factor decomposition and its connection to the estimation of load parameters under a steady-state regime, as described and discussed in the following sections.

### *4.1. Simulation Results*

The circuits shown in Figure 4 were carefully chosen to point out how very simple circuits/loads can be tricked in terms of the power phenomena interpretation and equivalent circuit modeling. For example, the circuits in Figure 4a,b represent two non-linear loads without energy storage elements (black box), but in the first one the current waveform lags with regard to the voltage signal, while in the second case, the voltage and current waveforms are in phase.

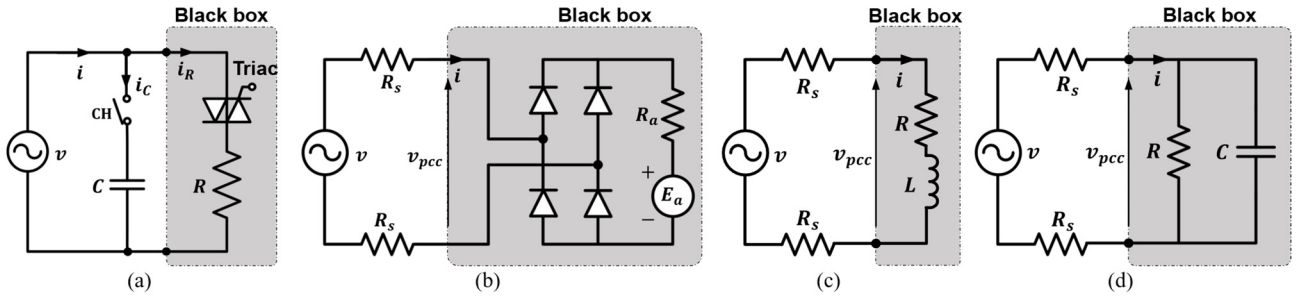


**Figure 4.** Circuits analyzed: (**a**) Resistive load controlled by Triac; (**b**) Non-linear load with voltage and current in phase; (**c**) Inductive-resistive (RL) load and (**d**) Capacitive-resistive (RC) load.

All the required algorithms and equations were digitally implemented in C++ language, assuming a sampling frequency of 12 kHz (200 samples per 60 Hz period), and the circuits were simulated using PSIM software.

Example #1: Figure 4a shows a resistive load ($R = 2\Omega$) with a Triac (firing angle $\alpha = 120^{o}$), which is supplied with $v = 127\sqrt{2}\sin(\omega_1 t)$ V and $\omega_1 = 377$ rad/s. The Triac-controlled circuit is considered an ideal device triggered by the "gating block" component from PSIM (triggering pulse model). Figure 5 shows the voltage, the current, and the resulting waveforms of the load-current terms and the corresponding equivalent circuit (EC) parameters estimation. Note that the current at PCC is decomposed into the active current $i_a$ (in phase with the voltage), which holds for the energy consumption; the void current $i_v$, occurs due to the nonlinearity introduced by the Triac and the reactive current $i_r$ (shifted by 90° with respect to the voltage), a characteristic that is not obvious because the load has no energy storage. Conventionally, reactive power/energy is associated with the presence of energy storage elements, with the intrinsic behavior of lead or lag in the current with respect to the voltage.

From the top of Figure 5, it is possible to notice that the fundamental component of the load current ($i_1$) lags the voltage waveform ($v$). Therefore, the reactive current occurs only because current $i_1$ and the voltage are phase-shifted, but not because of energy storage. Consequently, although a non-linear load might not have energy storage devices, it can produce reactive power/energy absorption associated with the non-linear behavior of the current waveform. Then, the simple asymmetry of the current waveform regarding the fundamental voltage peak is enough to characterize the phase shift of the fundamental current waveform. Thus, the reactive power/energy associated with the non-linear load is "inductive" when the current is delayed in comparison to the voltage reference or "capacitive" when the current is advanced regarding to that same reference.

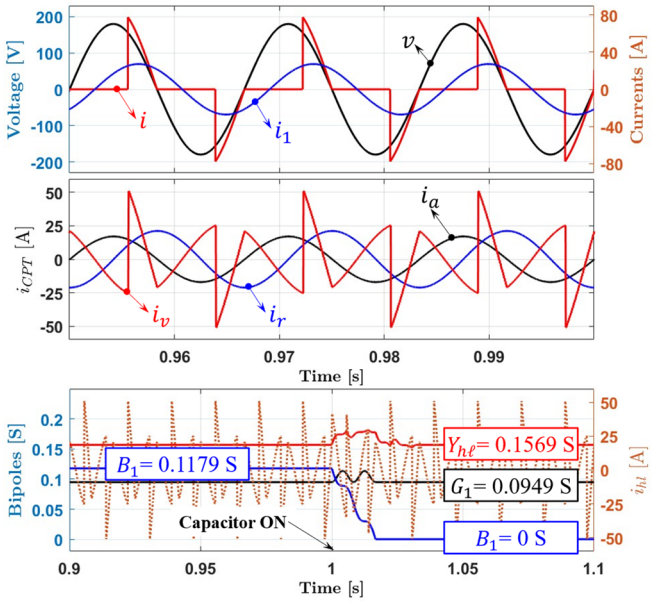


**Figure 5.** Example #1—Load modeling and characterization: voltage and current at PCC (**top**), current decomposition (**center**) and estimated load parameters (**bottom**).

Therefore, a resistive load controlled by Triac (Figure 4a) can be represented by a parallel EC in Figure 3a containing a conductance $G_1$, a susceptance $B_1$ and a load transadmittance $Y_{h\ell}$ (or a source of harmonic current $i_{h\ell}$). Thus, the load behaves as a "harmonic current source" type. The values of the EC dipoles which characterize the load are shown at the bottom of Figure 5. Since the voltage is sinusoidal, these values are identical to the equivalent values of the circuit in Figure 2, i.e., $G_e = G_1$, $B_e = B_1$ and $j_e = i_{h\ell}$ ($Y_e = Y_{h\ell}$).

From above, we conclude that it is necessary to re-evaluate the concept that reactive power/energy is eminently an oscillatory phenomenon between an energy storage element (inductors or capacitors) and the grid. Thus, as in Figure 4a, the inductive reactive power/energy represents the portion of fundamental energy that is demanded to satisfy the conditions of non-linearity. Namely, this "reactive power/energy" can be compensated by a shunt capacitor—other nonintuitive information. So, from (18) and the estimated value of $B_1$ (see the bottom part of Figure 5), such a capacitor at the fundamental frequency is equal to 312.73 µF.

Figure 5 (bottom) shows the values of the EC dipoles, while Table 1 summarizes the reactive energy and corresponding load power terms at PCC before and after compensation. Notice that the estimated value of $B_1$ becomes zero after turning ON the capacitor, and as a result, the reactive power/energy is entirely compensated. Moreover, from the grid point of view, the capacitor does not affect the active power $P$ and distortion power $D$, since the conductance $G_1$ and the load transadmittance $Y_{h\ell}$ (harmonic current of the load $i_{h\ell}$) remain unchanged, corroborating the fact that the power/current terms are orthogonal. Therefore, the intervention of the capacitor reduces the apparent power and improves the power factor from 0.4359 to 0.518.

**Table 1.** Example #1—Power Terms and Reactive Energy at PCC.

| $A$ [VA] | $P$ [W] | $Q$ [var] | $D$ [VA] | $W_r$ [J] | |
|---|---|---|---|---|---|
| 3514.991 | 1532.054 | 1899.209 | 2530.015 | 5.0437 | Without C |
| 2957.425 | 1531.978 | 0.000 | 2529.704 | 0.0000 | With C |

In conclusion, the reactive energy not only relates to the energy exchange between the source and the energy storage elements [12,35], but it has a broader meaning: that is, regardless of what promotes it (either electromagnetic fields present in inductors and

electric fields in capacitors or electronic switching), the reactive power/energy is associated with the voltage and current lead/lag at each frequency.

Example #2: Figure 4b shows a non-linear load on which the voltage and current waveforms are in phase. The equivalent circuit represented by $R_a = 0.2\ \Omega$, $E_a = 127$ V is fed by a single-phase ideal full-wave rectifier. The non-linear load is supplied with a sinusoidal voltage (identical to Example #1), through a purely resistive line impedance $R_s = 0.4\ \Omega$.

Figure 6 shows the waveforms of the voltage, current, load-current terms, and the results of the EC parameters estimation. Note that, differently from example #1, the fundamental current $i_1$ is in phase with the voltage $v$. Hence, the reactive energy/power results in zero. This statement can be confirmed by the zero reactive ($i_r$) current at the center of Figure 6. One can observe that due to the nonlinearity of the load, the component $i_v$ is not negligible. Furthermore, $i_v$ (distortion current) flows through the line impedance, and as a result, the voltage at PCC is distorted (see Figure 6, top). In fact, the $THD_I$ is 60.43%, which leads to $THD_V = 10.27\%$.

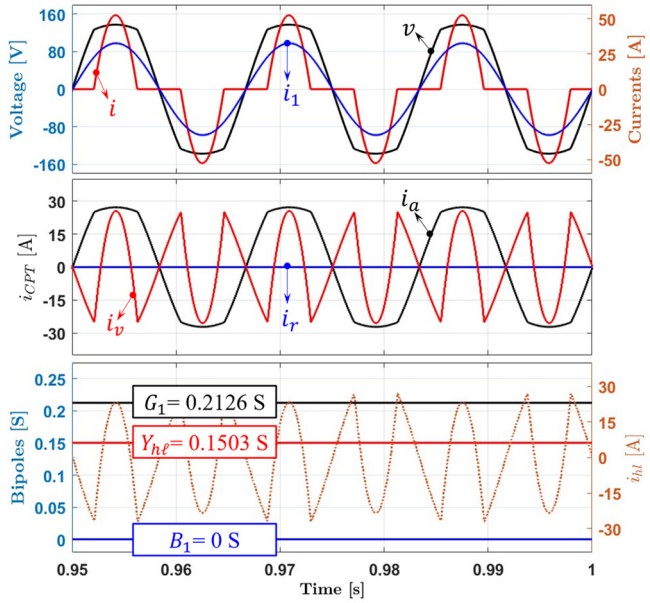


**Figure 6.** Example #2–Load modeling and characterization: voltage and current at PCC (**top**), current decomposition (**center**) and estimated load parameters (**bottom**).

Since the load does not represent any circulation of reactive energy, it can be characterized by an EC contend with only a fundamental conductance $G_1$ and a harmonic current source $i_{h\ell}$ (or a load transadmittance $Y_{h\ell}$). According to this notion, the circuit of Figure 4b behaves as a harmonic current source (parallel association as in Figure 3a). The estimated parameters of the EC are shown at the bottom of Figure 6.

Another important concern of load characterization is identifying which portions of apparent power can be used for revenue metering. Usually, the integral of the active power ($P$) for a certain period is used (kWh). However, it is known that this quantity includes a portion of harmonic active power, leading to the question of whether this portion should or should not be included in the energy bill.

Table 2 shows power terms, reactive energy, and load conformity factors at PCC. Observe that the fundamental active power is greater than the total active power ($P_1 > P$). In this regard, it is interesting to analyze the active power components in the frequency domain:

$$P = P_1 + \sum_{h=2}^{\infty} P_h = P_1 + P_H \tag{28}$$

where $P_H$ is the harmonic active power. Thus, from Table 2 and (28), $P_H$ results:

$$P_H = P - P_1 = V_H I_H = 23.489 - 25.045 \cong -1.556\text{kW}$$

while the fundamental active power $P_1$ is positive, the harmonic active power $P_H$ is negative. The negative value means that the harmonic active power (i.e., generated by the load) returns from the load to the grid, and this energy is dissipated over the line impedance ($P_H = -R_S I_H^2$), increasing the losses. Since the voltage source is sinusoidal, $P_H$ is supplied to the load through the fundamental component, and therefore, $P_1$ is greater than $P$. In fact, harmonic currents generated in the load cause the flow of $P_H$. Therefore, it can be said that $P_1$ supplies the useful power $P$ of the load and the losses associated with the harmonics $P_H$ (load with frequency converter characteristics).

**Table 2.** Example #2—Power Terms and Conformity factors at PCC.

| $A$ [VA] | $P$ [W] | $Q$ [var] | $D$ [VA] | $W_r$ [J] | $P_1$ [W] |
|---|---|---|---|---|---|
| 2941.180 | 2348.981 | 0.000 | 1771.018 | 0.000 | 2504.537 |
| | $\lambda$ | $\lambda_Q$ | $\lambda_D$ | | |
| | 0.799 | 0.000 | 0.602 | | |

From the above analysis, it is clear that $P_1$ is the power required for the load to work properly; as a result, for billing purposes, the customer (load) must be charged for the energy associated with this power, i.e.,:

$$kWh = \int_0^{month} P_1 dt \tag{29}$$

In effect, (29) provides not only the information of the energy delivered to the non-linear load but also the additional energy dissipated in the distribution system originated from the load itself. Such an accountability method was suggested by the authors of this paper in [33].

Finally, to evaluate qualitatively the effects of the harmonics on the active power, using $P_H$ and $P_1$, a new index can be defined as:

$$\lambda_P = \frac{P_H}{P_1} = \lambda \frac{A}{P_1} - 1 \tag{30}$$

which refers to a nonconformity factor of the active power and shows how much-undesired power generating harmful effects is contained on the active power. Factor $\lambda_P$ is due to the distortion voltage and it vanishes only if the voltage at the PCC is sinusoidal, leading to $P_1 = P$. Consequently, 10.27% of $THD_V$ originated from the load causes 6.21% additional line losses ($\lambda_P = -0.0621$).

Example #3: Figure 4c shows a $RL$ load representing an induction motor per-phase equivalent circuit in steady-state (3 kW, cos$\phi$ = 0.8, $R$ = 3.441 Ω and $L$ = 6.845 mH), supplied from a source of non-sinusoidal voltage and $R_s$ = 0.4 Ω. The supply voltage is as in Example #1, added by 10% of the 3rd and 5th harmonics.

Figure 7 shows the waveforms of the voltage, current, load-current terms, and results of the EC parameters estimation. It is observed that, besides the active ($i_a$) and reactive ($i_r$) current, there is also the void ($i_v$) current caused by the nonlinearity between the waveforms of the voltage (source) and current (inductive load). In fact, the $THD_V$ (15.86 %) imposed by the source promoted 6.71% of $THD_I$.

As expected, the load estimated parameters shown at the bottom of Figure 7 indicate that the circuit of Figure 4c behaves as a harmonic current source ($W_r > 0$). So, the EC is composed by a parallel association of $G_1$, $B_1$ and, current source $i_{h\ell}$ (or a load transadmittance $Y_{h\ell}$) as Figure 3a. Furthermore, the equivalent estimated values, i.e., $G_1 \parallel B_1 = Y_{e1} = \frac{1}{Z_{e1}} \Rightarrow Z_{e1} = 3.440 + \text{j}2.582\ \Omega$, with $\phi = 36.883^\circ$ are close to the induction motor equivalent circuit parameters. Therefore, such estimated values of the EC represent a good estimation of the load parameters.

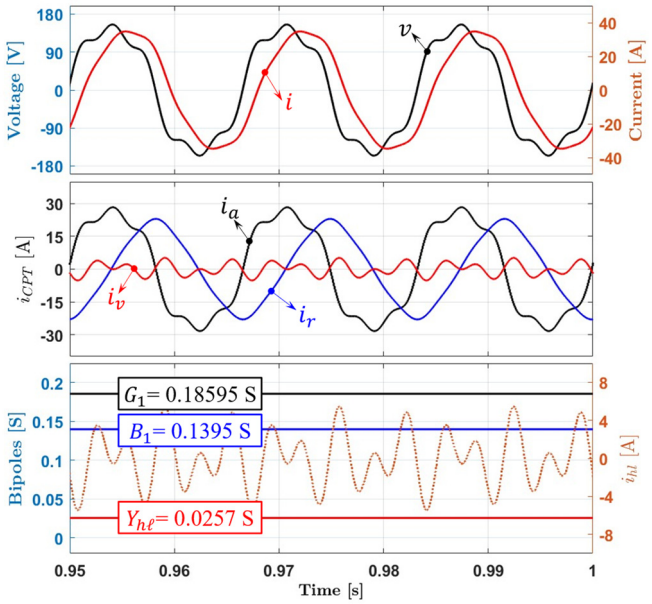


**Figure 7.** Example #3—Load modeling and characterization: voltage and current at PCC (**top**), current decomposition (**center**) and estimated load parameters (**bottom**).

The revenue metering is also analyzed, and Table 3 shows the results of power terms, reactive energy, and corresponding load conformity factors at PCC.

**Table 3.** Example #3—Power Terms and Conformity factors at PCC.

| $A$ [VA] | $P$ [W] | $Q$ [var] | $D$ [VA] | $W_r$ [J] | $P_1$ [W] |
|---|---|---|---|---|---|
| 2856.440 | 2262.096 | 1715.995 | 312.298 | 4.481 | 2251.391 |
| | $\lambda$ | $\lambda_Q$ | $\lambda_D$ | $\lambda_P$ | |
| | 0.7919 | 0.6044 | 0.1093 | 0.005 | |

From (28) and Table 3, the power $P_H$ results:

$$P_H = P - P_1 = 2262.096 - 2251.391 = 10.705\text{W}$$

Unlike example #2 (non-linear load), the harmonic active power is positive, indicating that the harmonic active power (generated by the source) is absorbed by the load, then $P_1$ results lower than $P$. Thus, it can be said that the useful work produced by $P_1$ is lower than the total active power supplied $P$, due to the harmonic active power in the feeder which is positive ($P_H = R_S I_H^2$).

Since the voltage source supplies $P_H$ to the load, the consumer (load) should be charged only for the energy associated with the power needed for its operation (useful power), namely, the fundamental active energy (29). Indeed, only fundamental active power transfers useful power to the induction motor, $P_1 = P - P_H$. Moreover, the harmonics generated by the source are absorbed by the magnetic field of the inductor, modifying the amplitude and phase of the harmonic components imposed by the source and generating a distortion power ($D = 312.298$ VA), which increases the losses in the line.

Following this approach, the active power $P$ can be re-evaluated by considering the sign of harmonic active power $P_H$, which is due to the distortion caused by the load and source, thus:

$$P = \frac{1}{T}\int_0^T vidt = P_1 \pm \sum_{h=2}^{\infty} P_h = P_1 \pm P_H \tag{31}$$

Observe now that $P_H$ can be positive or negative, indicating that the harmonic active power flow is from the source to the load (+), or from the load to the source (−). It is worth noting that (31) gives a proper evaluation of the active power in the assumption that the

load behaves either as a harmonic current generator or not. Hence, the total active power $P$ could be smaller or larger than the fundamental active power $P_1$ measured at PCC.

In addition, from (30) and (31), $\lambda_P$ is greater than zero (+) when the harmonic active power flow is originated by the power supply or smaller than zero (−) when the harmonic active power is caused by the load. Consequently, $\lambda_P$ can be taken as an index to indicate the direction of the harmonic active power flow. So, according to (30), $\lambda_P$ results are slightly higher than zero (0.005), suggesting that the harmonic flow comes from the source to the load; then the additional line losses caused by the voltage source are 0.5%.

Example #4: Figure 4d shows the resistive-capacitive ($R = 1\Omega$ and $C = 1989.2$ μF) load, which is considered under two supply conditions, sinusoidal as in Example #1, and non-sinusoidal, as in Example #3. The line impedance $R_s$ is considered as 1.8 $m\Omega$, and in the case of sinusoidal voltage, three different operating frequencies were considered: 60, 55 and, 63 Hz.

Case I: Table 4 shows power terms, reactive energy, and load conformity factors at PCC. As expected for sinusoidal voltage conditions, only active ($P$) and reactive ($Q$) power are demanded from the source. The capacitive nature of the load is evidenced by the negative values of $W_r$ and $Q$. Otherwise, according to (8), the reactive power under sinusoidal voltage conditions results in $Q = \omega W_r$. This is confirmed by the results shown in Table 4 (Case I). It is worth noticing that the apparent power $A$ and the reactive power $Q$ are influenced by the line frequency variation. In contrast, the active power $P$ and reactive energy $W_r$ remain constant, i.e.,

$$A^{60} \neq A^{55} \neq A^{63} \text{ and } Q^{60} \neq Q^{55} \neq Q^{63}$$

$$W_r^{60} = W_r^{55} = W_r^{63} = -29.873 \text{ J}$$

$$P^{60} = P^{55} = P^{63} = 15.017 \text{ kW}$$

**Table 4.** Example #4—Power Terms and Conformity factors at PCC.

| | | **Case I** | | **Case II** |
|---|---|---|---|---|
| $f_1$ [Hz] | 60 | 55 | 63 | 60 |
| $A$ [VA] | 18,771.043 | 18,223.401 | 19,114.199 | 20,180.949 |
| $P$ [W] | 15,017.343 | 15,017.343 | 15,017.343 | 15,314.472 |
| $Q$ [var] | −11,261.948 | −10,323.359 | −11,825.059 | −11,589.153 |
| $D$ [VA] | 0 | 0 | 0 | 6199.129 |
| $W_r$ [J] | −29.873 | −29.873 | −29.873 | −30.464 |
| $P_1$ [W] | 15,017.398 | 15,017.398 | 15,017.398 | 15,017.398 |
| $P_H$ [W] | 0 | 0 | 0 | 297.074 |
| $\lambda$ | 0.8000 | 0.8144 | 0.7856 | 0.7589 |
| $\lambda_Q$ | 0.6000 | 0.5802 | 0.6187 | 0.6034 |
| $\lambda_D$ | 0 | 0 | 0 | 0.3072 |
| $\lambda_P$ | 0 | 0 | 0 | 0.0198 |

Thus, while active power $P$ and reactive energy $W_r$ are conservative, reactive power $Q$ and apparent power $A$ are not conservative.

Case II: Under non-sinusoidal supply voltage, similarly to inductive load (Example #3) the resistive-capacitive load not only demands reactive power $Q$ but also distortion $D$ power from the source. In effect, the harmonics generated by the source are absorbed by the electric field of the capacitor modifying the amplitude and phase of the harmonic components imposed by the source generating a not negligible distortion power ($D = 6199.129$ VA) which increases the losses in the line. In this case, the $THD_V$ (14.07%) imposed by the source promotes 36.53% of $THD_I$.

The data relating to the case of non-sinusoidal condition are given in Table 4, and Figure 8 shows that voltage distortion produces a high current ($i$) distortion, a slightly reactive current ($i_r$) distortion, and a significant void current ($i_v$).

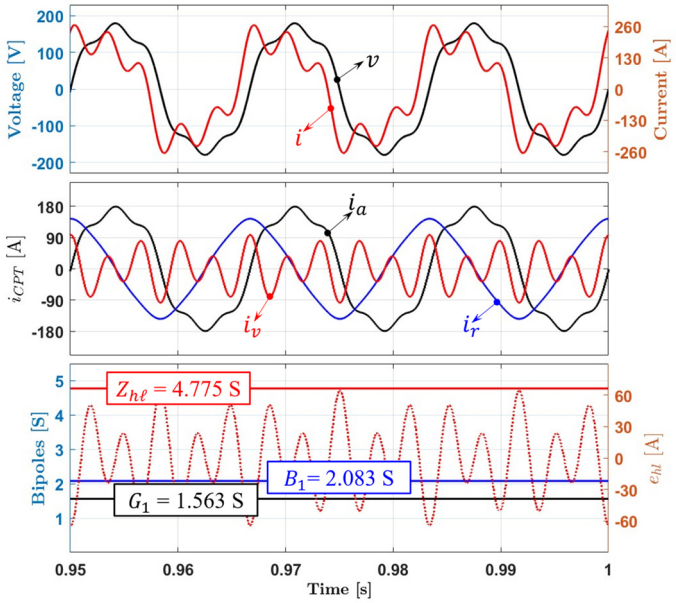


**Figure 8.** Example #4 Case II—Load-modeling and load-characterization: voltage and current at PCC (**top**), current decomposition (**middle**) and estimated load parameters (**bottom**).

Unlike Case I, note that the product of the angular frequency by the reactive energy is different from the reactive power ($\omega W_r \neq Q$). In fact, reactive power $Q$ depends on the voltage distortion and angular line frequency as shown in (8). Besides, it is worth mentioning that both active ($P$) and reactive ($Q$) powers include the contributions from harmonic components, as shown in Table 4.

Similar to Example #3, the revenue metering can be analyzed based on the values of Table 4. Note that the harmonic active power flow in a load with a capacitive nature also results positively, i.e., $P_H = 15.3145 - 15.0174 \cong 0.2971$ kW, indicating that $P_H$ is absorbed by the load. Then the active power is larger than the fundamental active power ($P = P_1 + P_H \Rightarrow P > P_1$). In this way, the customer (load) consumption should be also charged according to (29), i.e., again the fundamental active energy. In addition, it is observed that $\lambda_P$ is positive (0.0198), suggesting that the harmonic active power flow is generated by the power supply. In this case, 14.07% of $THD_V$ causes 1.98% of additional losses in the line.

Finally, estimated parameters of the load are shown at the bottom of Figure 8. As expected, the proposed approach indicates that the circuit of Figure 4d behaves as a harmonic voltage source ($W_r < 0$). Correspondingly, the EC is composed of a series association of $G_1$, $B_1$ and voltage source $e_{h\ell}$ (or a load transimpedance $Z_{h\ell}$) as in Figure 3b. Furthermore, the equivalent estimated values, i.e., $Y_{e1} = G_1 + jB_1$, are close to the resistive-capacitive load parameter, i.e., $R \parallel X_C = 0.64 - j0.4799\ \Omega$. Therefore, estimated values of the EC represent a good estimation of the load parameters.

### *4.2. Experimental Results*

To experimentally validate the estimation of the proposed load parameters, a digital oscilloscope (analog bandwidth of 100 MHz; maximum sample rate of 2.5 GS/s; input sensitivity range of 1 mV/div; vertical resolution of 11 bits; DC gain accuracy ±1.5%), with compensated hall effect current probes (frequency range DC to 100 kHz) and high voltage-active differential probes (bandwidth of 50 MHz and attenuation 50×/500×) was used for measuring a set of two residential loads. Then, considering a dataset corresponding to 6 cycles of fundamental frequency, the EC estimated parameters were calculated with Matlab software.

Example #5—Compact fluorescent lamp: Considering the approach of Section 3, Figure 9 shows the results of the load parameter estimation and the corresponding voltage

$v$ and current $i$ at PCC. Note a slight voltage distortion (2%) and very high current distortion ($DHT_I = 143.52\%$), which can also be confirmed by the small difference between the active power $P$ and its fundamental component $P_1$, a high distortion power $D$ and a low power factor in Table 5.

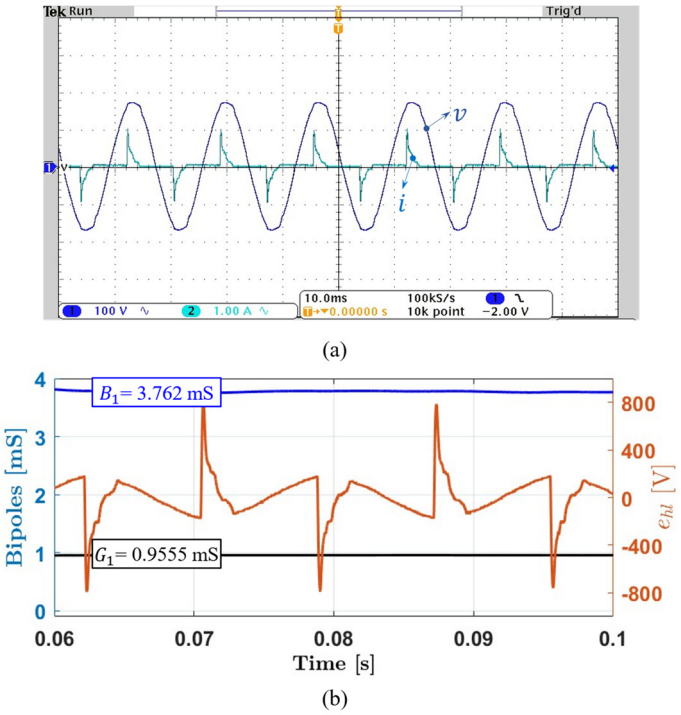


**Figure 9.** Example #5: compact fluorescent lamp. (**a**) measured voltage and current waveforms; (**b**) estimated load parameters.

**Table 5.** Example #5: compact fluorescent lamp—Power Terms and Conformity factors at PCC.

| $A$ [VA] | $P$ [W] | $Q$ [var] | $D$ [VA] | $W_r$ [J] | $P_1$ [W] |
|---|---|---|---|---|---|
| 24.1172 | 13.4568 | −3.3965 | 19.7246 | −0.0090 | 13.4617 |
| | $\lambda$ | $\lambda_Q$ | $\lambda_D$ | $\lambda_P$ | |
| | 0.5580 | 0.2447 | 0.8179 | −0.0004 | |

When the nature of the load is considered, it can be foreseen that the approach will work properly, as confirmed by the results in Table 5 and in Figure 9b, showing a negative reactive energy/power and the estimated parameters of the load ($R_1$, $C_1$ and $e_{h\ell}$). Therefore, the fluorescent lamp can be modeled by an HVS as in Figure 3b, where the series EC is constituted by $R_1$ (1.0465 kΩ), $C_1$ (9.98 μF) and a harmonics voltage source $e_{h\ell}$ (see Figure 9b), representing the harmonics generated by the fluorescent lamp (non-linear load). Moreover, based on the nonconformity factor of the active power ($\lambda_P$), one can observe that the harmonic active power flow in a load with the HVS characteristic is negative, suggesting that the harmonic active power flow is generated by the load. Therefore, as the fundamental active power results are slightly larger than active power ($P_1 > P$) from the revenue-metering point of view, the load consumption should be charged by the fundamental component, i.e., according to (29). In addition, as the $THD_V$ is low (2%), the distortion factor ($\lambda_D$) is equivalent to the $THD_I$ i.e., $\lambda_D = 0.8179 \cong \frac{1.4352}{\sqrt{1+1.4352^2}} = 0.8205$. Thus, although the compact fluorescent lamp has a high displacement factor ($\lambda_Q = 0.2447 \cong \sin\phi \Rightarrow \cos\phi = 0.9696$), due to the HVS characteristic (capacitive behavior), the power factor results are very low ($\lambda = 0.558$) and a high distortion factor (82%) is observed.

Example #6—Fan operating at full speed: Figure 10 shows the voltage ($v$) and current ($i$) waveforms and the resulting estimated load parameters. In this case, the $THD$ of the voltage and current waveforms is 3.3% and 24.79%, respectively. As expected, due to the inductive nature of the load, the reactive energy/power results are positive (see Table 6). Thus, the fan behaves like an HCS (as in Figure 3a), and its EC can be represented by a parallel configuration of a $R_1$ (100.18 Ω), a $L_1$ (986.245 mH), and a harmonic current source $j_{h\ell}$, representing the harmonics generated by the fan. Similar to the previous example, the revenue metering and power quality issues can be analyzed based on the values of Table 5. Unlike the HVS load type in a load with HCS characteristics, the active power is slightly larger than the fundamental active power ($P > P_1$), indicating that the harmonic active power is absorbed by the load ($\lambda_P$ is positive), then the load consumption should be also charged by the fundamental component, i.e., according to (29). In addition, due to the HCS characteristics (inductive behavior), the distortion factor results are low (24 %) when compared to the load type HVS (capacitive behavior), i.e., $\lambda_D = 0.2382 \cong \frac{0.2479}{\sqrt{1+0.2479^2}} = 0.2406$. Thus, the displacement factor and power factor results are relatively high, i.e., $\lambda_Q = 0.2594 \cong \sin\phi \Rightarrow \cos\phi = 0.9658$ and $\lambda = 0.938$.

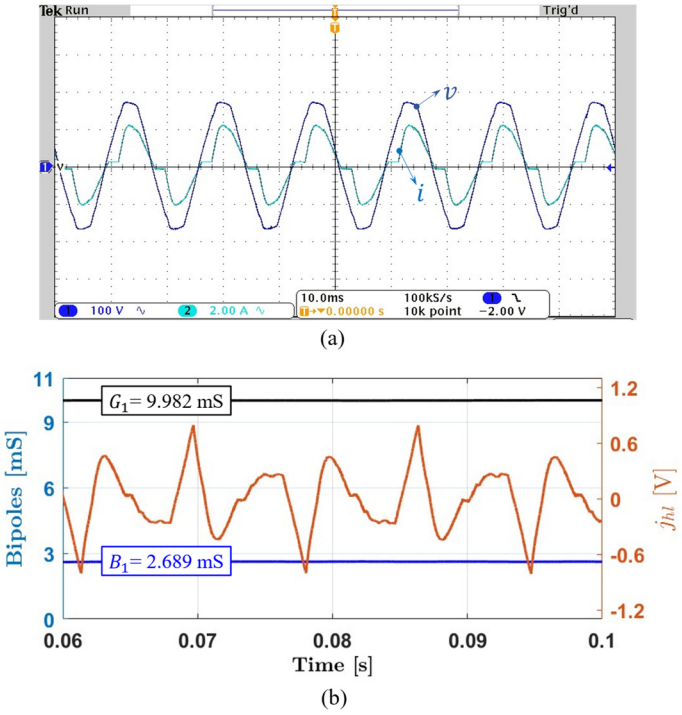


**Figure 10.** Example #6: fan at full speed. (**a**) measured voltage and current waveforms; (**b**) estimated load parameters.

**Table 6.** Example #6 fan at Full Speed—Power Terms and Conformity Factors.

| $A$ [VA] | $P$ [W] | $Q$ [var] | $D$ [VA] | $W_r$ [J] | $P_1$ [W] |
|---|---|---|---|---|---|
| 159.956 | 150.035 | 40.301 | 38.105 | 0.1069 | 149.491 |
| | $\lambda$ | $\lambda_Q$ | $\lambda_D$ | $\lambda_P$ | |
| | 0.9380 | 0.2594 | 0.2382 | 0.0036 | |

It is important to point out that the obtained results can be influenced by measurement errors and uncertainties, as in any other power theory measure-based modeling approach; however, different strategies can be applied for minimizing such influences [41], as demonstrated in some previous experimental investigations [42–44].

## 5. Conclusions

This paper proposes a new theoretical background for the analysis of single-phase electrical systems operating under non-ideal conditions. The paper particularly stresses the practical conditions related to weak grids, such as in microgrids where the above-mentioned non-idealities become more relevant and circuits can also operate in islanded mode, and where considerable voltage distortions and frequency variations may occur.

The proposed approach was based on the Conservative Power Theory and results in a powerful technique for estimating equivalent circuit (EC) parameters capable of representing linear or non-linear (generic) loads under sinusoidal or distorted voltage conditions by means of passive dipoles or voltage/current harmonic sources (active dipoles) and intrinsic transimpedance or transadmittance.

Among other discussed possibilities, such as power factor compensation, the proposed method allows approaching another aspect of great relevance in power systems with deteriorated voltages, the accountability problem. The identification of supply and load responsibility regarding reactive and harmonic currents is, in fact, a problem of primary importance for a proper revision of revenue metering methods in modern (micro) grids.

To validate the proposed method, computer simulations and experimental tests were performed, assuming different circuits and supply conditions. The simulation results demonstrate that the estimated parameters for the equivalent circuit practically match the values from simulations, while the nonlinearities are modeled by estimated harmonic current or voltage sources. Moreover, the simulations also provide important information about the origins of reactive and void power/current terms in different operating circuits and conditions, and their respective effect on power factor calculation and compensation, as well as about the analysis of harmonic power flow and its impact in revenue metering. The results show that a proper method for charging consumers should be based on measuring the PCC energy absorbed at the fundamental frequency. In this way, the non-linear loads would pay for both the power drained and for the harmonic losses imposed into the grid. In the case of linear loads (except pure resistive load), consumers would be paying just by the useful drained power. Therefore, the total active power ($P = P_1 + P_H$) represents useful power only in case of pure resistive load. In any other linear load, useful power is related to the fundamental active power ($P_1$).

In contrast, experimental results reveal that the proposed method can estimate passive and active parameters for modeling the real loads as equivalent circuits, which properly represent the power phenomena of generic single-phase nonlinear loads in real operating conditions. Apart from providing information for discussing responsibility assessment for revenue metering or power quality analyses, such equivalent parameters might also be useful for more complex studies and computer simulations, such as the development of digital twins for smart grid applications.

Consequently, the estimation of load parameters and revenue metering approaches have been described and validated as a method of both theoretical and practical interest. Likewise, the proposed approaches can be easily implemented in digital platforms, setting the basis for possible retrofits or new technologies for energy and power quality meters, power electronics-based power conditioners, energy management systems, and other applications. In future works, the authors intend to extend the proposed methodology to scenarios with distributed energy sources and three-phase circuits.

**Author Contributions:** Conceptualization: H.K.M.P. and F.P.M.; methodology: H.K.M.P., F.A.S.G. and F.P.M.; validation: H.K.M.P., M.B.A. and A.C.M.; Formal analysis: H.K.M.P., M.B.A., A.C.M., F.A.S.G. and F.P.M.; writing, review and editing: H.K.M.P., M.B.A., A.C.M., F.A.S.G. and F.P.M.; funding acquisition: H.K.M.P. All authors have read and agreed to the published version of the manuscript.

**Funding:** The authors are grateful to the São Paulo Research Foundation (FAPESP) (Grants 2016/08645-9), the National Council for Scientific and Technological Development (CNPq) (Grant 309297/2021-4) and in part the Coordination for the Improvement of Higher Education Personnel (CAPES) under Finance Code 001.

**Data Availability Statement:** Not applicable.

**Conflicts of Interest:** The authors declare no conflict of interest. The funders had no role in the design of the study; in the collection, analyses, or interpretation of data; in the writing of the manuscript; or in the decision to publish the results.

## Acronyms and Notation

| | |
|---|---|
| AC | Alternating Current |
| CPT | Conservative Power Theory |
| DC | Direct Current |
| EC | Equivalent Circuits |
| HCS | Harmonic Current Source |
| HVS | Harmonic Voltage Source |
| PCC | Point of Common Coupling |
| PQ | Power Quality |
| RMS | Root Mean Square |
| $THD_I$ | Current Total Harmonic Distortion |
| $THD_V$ | Voltage Total Harmonic Distortion |
| $e_{hl}$ | Voltage Source |
| $f_1$ | Fundamental Frequency |
| $h$ | Harmonic Order |
| $\hat{i}$ | Unbiased Current Integral |
| $i_1$ | Fundamental Current |
| $i_a$ | Active Current |
| $\hat{i}_h$ | Unbiased Harmonic Current Integral |
| $i_h$ | Harmonic Current |
| $i_{hl}$ | Harmonic Current Source |
| $i_l$ | Current Accountable to the Load |
| $i_r$ | Reactive Current |
| $i_v$ | Void Current |
| $j_e$ | Harmonic Current Source |
| $u_e$ | Harmonic Voltage Source |
| $\hat{v}$ | Unbiased Voltage Integral |
| $v_1$ | Fundamental Voltage |
| $v_a$ | Active Voltage |
| $\hat{v}_h$ | Unbiased Harmonic Voltage Integral |
| $v_h$ | Harmonic Voltage |
| $v_{hl}$ | Harmonic Voltage Source |
| $v_r$ | Reactive Voltage |
| $v_v$ | Void Voltage |
| $\lambda$ | Power Factor |
| $\lambda_D$ | Non-linearity Factor |
| $\lambda_Q$ | Reactivity Factor |
| $\lambda_P$ | Nonconformity Factor of the Active Power |
| $\omega$ | Angular Line Frequency |
| $\sigma_i$ | Current Distortion Factor |
| $\sigma_v$ | Voltage Distortion Factor |
| $A$ | Apparent Power |
| $B_1$ | Fundamental Equivalent Susceptance |
| $B_{C1}$ | Fundamental Capacitive Susceptance |
| $B_{eC}$ | Capacitive Equivalent Susceptance |
| $B_{eL}$ | Inductive Equivalent Susceptance |
| $B_{L1}$ | Fundamental Inductive Susceptance |
| $C_1$ | Capacitor at Fundamental Frequency |
| $C_e$ | Equivalent Capacitance |
| $D$ | Distortion Power |
| $G_1$ | Fundamental Equivalent Conductance |

| | |
|---|---|
| $G_e$ | Equivalent Conductance |
| $I$ | RMS Value of Current |
| $I_a$ | RMS Value of $i_a$ |
| $I_{hl}$ | RMS Value of the Harmonic Current Generated by the Load |
| $I_r$ | RMS Value of $i_r$ |
| $I_v$ | RMS Value of $i_v$ |
| $L_1$ | Fundamental Inductance |
| $L_e$ | Equivalent Inductance |
| $P$ | Active Power |
| $P_1$ | Fundamental Active Power |
| $P_h$ | Harmonic Active Power |
| $Q$ | Reactive Power |
| $Q_1$ | Fundamental Reactive Power |
| $R_1$ | Fundamental Resistance |
| $R_e$ | Equivalent Resistance |
| $R_s$ | Resistive Line Impedance |
| $V$ | RMS Value of the Voltage |
| $\hat{V}$ | RMS Value of $\hat{v}$ |
| $V_1$ | RMS Value of $v_1$ |
| $V_a$ | RMS Value of $v_a$ |
| $V_r$ | RMS Value of $v_r$ |
| $V_v$ | RMS Value of $v_v$ |
| $W_r$ | Reactive Energy |
| $W_{r1}$ | Reactive Energy at Fundamental Frequency |
| $Y_e$ | Equivalent Admittance |
| $Y_{e1}$ | Fundamental Equivalent Admittance |
| $Y_{ei}$ | Equivalent Transadmittance |
| $Y_{li}$ | Load Transadmittance |
| $Z_{ev}$ | Equivalent Transimpedance |
| $Z_{hl}$ | Load Transimpedance |

## Appendix A

The CPT authors define the unbiased time integral [9]:

$$\hat{x} = x_{\int} - x_{\int} = \int_0^t x(\tau)d\tau - \frac{1}{T}\int_0^T \left[\int_0^t x(\tau)d\tau\right] dt. \tag{A1}$$

where $x$ can represent the voltage, $v$, or the current, $i$ and $x_{\int}$ is the integral of $x$ and $x_{\int}$ is the average value of $x_{\int}$. So, the RMS value of $\hat{x}$ can be written as:

$$\hat{X} = \sqrt{\sum_{h=1}^{\infty} \hat{X}_h^2} = \sqrt{\sum_{h=1}^{\infty} \frac{X_h^2}{\omega^2 h^2}}, \tag{A2}$$

where $\omega$ is the fundamental angular frequency and $h$ indicates the harmonic order.

Using the definition of total harmonic distortion ($THD$), it is possible to define the relation between the RMS values of $x$ and $\hat{x}$, such as:

$$\frac{X}{\hat{X}} = \omega\sqrt{\frac{1+THD_x^2}{1+THD_{\hat{x}}^2}}, \tag{A3}$$

where $THD_x = \sum_{h=2}^{\infty} X_h/X_1$ is the total harmonic distortion of $x$ and $THD_{\hat{x}} = \sum_{h=2}^{\infty} \hat{X}_h/\hat{X}_1$ is the weighted total harmonic distortion of $x$ (voltage or current).

Therefore, we can define the voltage or current distortion factor to be:

$$\sigma_x = \sqrt{\frac{1+THD_x^2}{1+THD_{\hat{x}}^2}} - 1. \tag{A4}$$

Finally, from (A3) and (A4) we have:

$$\frac{X}{\hat{X}} = \omega(1 + \sigma_v). \tag{A5}$$

Since $THD_x^2 \geq THD_{\hat{x}}^2$, the distortion factor is always greater than or equal to zero ($\sigma_x \geq 0$). Moreover, if $\sigma_x = 0$, the effective voltage or current values and their unbiased time integral can be associated by the angular frequency ($X = \omega\hat{X}$).

## References


1. Bollen, M.H.J.; Das, R.; Djokic, S.; Ciufo, P.; Meyer, J.; Ronnberg, S.K.; Zavodam, F. Power Quality Concerns in Implementing Smart Distribution-Grid Applications. *IEEE Trans. Smart Grid* **2017**, *8*, 391–399. [CrossRef]
2. Muscas, C. Power quality monitoring in modern electric distribution systems. *IEEE Instrum. Meas. Mag.* **2010**, *13*, 19–27. [CrossRef]
3. Moreira, A.C.; Paredes, H.K.M.; De Souza, W.A.; Marafão, F.P.; Da Silva, L.C.P. Intelligent Expert System for Power Quality Improvement Under Distorted and Unbalanced Conditions in Three-Phase AC Microgrids. *IEEE Trans. Smart Grid* **2018**, *9*, 6951–6960. [CrossRef]
4. *P519.1/D12*; IEEE Draft Guide for Applying Harmonic Limits on Power Systems. IEEE Publisher: New York, NY, USA, 2015.
5. *519-2014*; IEEE Recommended Practice and Requirements for Harmonic Control in Electric Power Systems. IEEE Publisher: New York, NY, USA, 2014. [CrossRef]
6. Pomilio, J.A.; Deckmann, S.M. Characterization and compensation of harmonics and reactive power of residential and commercial loads. *IEEE Trans. Power Del.* **2007**, *22*, 1049–1055. [CrossRef]
7. Stathopoulos, T.; Alrawashdeh, H.; Al-Quraan, A.; Blockben, B.; Dilimulati, A.; Paraschivoiu, M.; Pilay, P. Urban wind energy: Some views on potential and challenges. *J. Wind. Eng. Ind. Aerodyn.* **2018**, *179*, 146–157. [CrossRef]
8. Al-Quraan, A.; Stathopoulos, T.; Pilay, P. Comparison of wind tunnel and on site measurements for urban wind energy estimation of potential yield. *J. Wind. Eng. Ind. Aerodyn.* **2016**, *158*, 1–10. [CrossRef]
9. Pomilio, J.A.; Bonaldo, J.P.; Morales-Paredes, H.K.; Tenti, P. About power factor and THDi in the smart micro-grid scenario. In Proceedings of the 2015 IEEE 13th Brazilian Power Electronics Conference and 1st Southern Power Electronics Conference (COBEP/SPEC), Fortaleza, Brazil, 29 November–2 December 2015; pp. 1–5. [CrossRef]
10. Emanuel, A.E. *Power Definitions and the Physical Mechanism of Power Flow*; John Wiley-IEEE Press: Hoboken, NJ, USA, 2010.
11. Akagi, H.; Watanabe, E.H.; Aredes, M. *Instantaneous Power Theory and Applications to Power Conditioning*; John Wiley-IEEE Press: Hoboken, NJ, USA, 2017.
12. Tenti, P.; Morales-Paredes, H.K.; Mattavelli, P. Conservative Power Theory, a Framework to Approach Control and Accountability Issues in Smart Microgrids. *IEEE Trans. Power Electron.* **2011**, *26*, 664–673. [CrossRef]
13. *1459-2010*; IEEE Standard Definitions for the Measurement of Electric Power Quantities Under Sinusoidal, Nonsinusoidal, Balanced and Unbalanced Conditions. IEEE Publisher: New York, NY, USA, 2010.
14. Steinmetz, C.P. *Theory and Calculation of Alternating Current Phenomena*; Kessinger Publishing: New York, NY, USA, 1897.
15. AIEE. Power Factor in Polyphase Circuit: Preliminary Report of the Special Joint Committee. *AIEE Trans.* **1920**, *39*, 1449–1520.
16. Fryze, S. Wirk, Blind, Scheinleistung: Elektrische Stromkreisen mit nichtsinusformingen Verlauf von Strom und Spannung. *ETZ* **1932**, *53*, 596–599.
17. Depenbrock, M. The FBD-Method, a Generally Applicable Tool for Analyzing Power Relations. *IEEE Trans. Power Syst.* **1993**, *8*, 381–387. [CrossRef]
18. Budeanu, C.I. *Puissances Reactives et Fictives*; Institute Romain de l'Energie: Bucharest, Romania, 1927.
19. Czarnecki, L.S. Currents' Physical Components (CPC) concept: A fundamental of power theory. In Proceedings of the 2008 International School on Nonsinusoidal Currents and Compensation, Lagow, Poland, 10–13 June 2008; pp. 1–11. [CrossRef]
20. León-Martínez, V.; Montañana-Romeu, J.; Peñalvo-López, E.; Valencia-Salazar, I. Relationship between Buchholz's Apparent Power and Instantaneous Power in Three-Phase Systems. *Appl. Sci.* **2020**, *10*, 1798. [CrossRef]
21. Shchurov, N.I.; Myatezh, S.V.; Malozyomov, B.V.; Shtang, A.A.; Martyushev, N.V.; Klyuev, R.V.; Dedov, S.I. Determination of Inactive Powers in a Single-Phase AC Network. *Energies* **2021**, *14*, 4814. [CrossRef]
22. Petrushyn, V.; Horoshko, V.; Plotkin, J.; Almuratova, N.; Toigozhinova, Z. Power Balance and Power Factors of Distorted Electrical Systems and Variable Speed Asynchronous Electric Drives. *Electronics* **2021**, *10*, 1676. [CrossRef]
23. De Almeida Coelho, R.; Brito, N.S.D. A new power calculation method based on time–frequency analysis. *Int. J. Electr. Power Energy Syst.* **2023**, *145*, 108709. [CrossRef]
24. Chica Leal, A.D.J.; Trujillo Rodríguez, C.L.; Santamaria, F. Comparative of Power Calculation Methods for Single-Phase Systems under Sinusoidal and Non-Sinusoidal Operation. *Energies* **2020**, *13*, 4322. [CrossRef]
25. Depenbrock, M.; Marshall, D.A.; Van Wyk, J.D. Formulating Requirements for a Universally Applicable Power Theory as Control algorithm in Power Compensator. *ETEP Eur. Trans. Electr. Power* **1994**, *4*, 445–454. [CrossRef]
26. Morales-Paredes, H.K.; Marafão, F.P.; Da Silva, L.C.P. A Comparative Analysis of FBD, PQ and CPT Current Decompositions–Part I: Three-phase, Three-Wire Systems. In Proceedings of the 2009 IEEE Bucharest PowerTech, Bucharest, Romania, 28 June–2 July 2009.

27. Marafão, F.P.; Morales-Paredes, H.K.; Da Silva, L.C.P. Critical Evaluation Of FBD, PQ and CPT Current Decompositions For Four-wire Circuits. *Eletronica De Potencia SOBRAEP* **2009**, *14*, 277–286. [CrossRef]
28. Marafao, F.P.; Liberado, E.V.; Morales-Paredes, H.K.; Da Silva, L.C.P. Three-phase four-wire circuits interpretation by means of different power theories. *Przegląd Elektrotechniczny* **2011**, *87*, 28–33.
29. Willems, J.L. Budeanu's Reactive Power and Related Concepts Revisited. *IEEE Trans. Instrum. Meas.* **2011**, *60*, 1182–1186. [CrossRef]
30. Peng, F.Z. Application Issues of Active Power Filters. *IEEE Ind. Appl. Mag.* **1998**, *4*, 21–30. [CrossRef]
31. Peng, F.Z. Harmonic Source and Filtering Approaches. *IEEE Ind. Appl. Mag.* **2001**, *7*, 18–25. [CrossRef]
32. Moreira, A.C.; Souza, W.A.; Conrado, B.R.P.; Morales-Paredes, H.K. Disturbing Load Classification Based on the Grey Relational Analysis Method and Load Performance Index. *J. Control. Autom. Electr. Syst.* **2020**, *31*, 141–152. [CrossRef]
33. Bonaldo, J.P.; Morales-Paredes, H.K.; Pomilio, J.A. Control of Single-Phase Power Converters Connected to Low Voltage Distorted Power Systems with Variable Compensation Objectives. *IEEE Trans. Power Electron.* **2015**, *31*, 2039–2052. [CrossRef]
34. Paredes, H.K.M.; Rodrigues, D.T.; Cebrian, J.C.; Bonaldo, J.P. CPT-Based Multi-Objective Strategy for Power Quality Enhancement in Three-Phase Three-Wire Systems Under Distorted and Unbalanced Voltage Conditions. *IEEE Access* **2021**, *9*, 53078–53095. [CrossRef]
35. Tenti, P.; Costabeber, A.; Mattavelli, P.; Marafão, F.P.; Morales-Paredes, H.K. Load Characterization and Revenue Metering Under Non-Sinusoidal and Asymmetrical Operation. *IEEE Trans. Instrum. Meas.* **2013**, *63*, 422–431. [CrossRef]
36. Morales-Paredes, H.K.; Marafão, F.P.; Da Silva, L.C.P.; Deckmann, S.M. Influence of Harmonics in Revenue Metering. In Proceedings of the Brazilian Conference on Power Quality (CBQEE), Santos, Brazil, 5–8 August 2007.
37. Xie, X.; Sun, Y. A piecewise probabilistic harmonic power flow approach in unbalanced residential distribution systems. *Int. J. Electr. Power Energy Syst.* **2022**, *141*, 108114. [CrossRef]
38. Montoya, F.G.; Baños, R.; Alcayde, A.; Arrabal-Campos, F.M. Analysis of power flow under non-sinusoidal conditions in the presence of harmonics and interharmonics using geometric algebra. *Int. J. Electr. Power Energy Syst.* **2019**, *111*, 486–492. [CrossRef]
39. Artale, G.; Caravello, G.; Cataliotti, A.; Cosentino, V.; Di Cara, D.; Guaiana, S.; Panzavecchia, N.; Tinè, G. Measurement of Simplified Single- and Three-Phase Parameters for Harmonic Emission Assessment Based on IEEE 1459-2010. *IEEE Trans. Instrum. Meas.* **2021**, *70*, 9000910. [CrossRef]
40. Paredes, H.K.M.; Marafão, F.; Mattavelli, P.; Tenti, P. Application of Conservative Power Theory to load and line characterization and revenue metering In Proceedings of the 2012 IEEE International Workshop on Applied Measurements for Power Systems (AMPS) Proceedings. Aachen, Germany, 26–28 September 2012; pp. 1–6.
41. Carstensa, H.; Xiaa, X.; Yadavallib, S. Measurement uncertainty in energy monitoring: Present state of the art. *Renew. Sustain. Energy Rev.* **2018**, *82*, 2791–2805. [CrossRef]
42. Arenas, L.O.; Melo, G.A.; Canesin, C.A. A Methodology for Power Quantities Calculation Applied to an FPGA-Based Smart-Energy Meter. *IEEE Trans. Instrum. Meas.* **2021**, *70*, 9000711. [CrossRef]
43. Tenti, P.; Paredes, H.K.M.; Marafão, F.P.; Mattavelli, P. Accountability in Smart Microgrids Based on Conservative Power Theory. *IEEE Trans. Instrum. Meas.* **2011**, *60*, 3058–3069. [CrossRef]
44. Marafão, F.P.; Souza, W.A.; Liberado, E.V.; Silva, L.C.P.; Paredes, H.K.M. Load Analyser using Conservative Power Theory. *Przegląd Elektrotechniczny* **2013**, *89*, 1–6.